

Precision calculation of isospin-symmetry-breaking corrections to $T = 1/2$ mirror decays using multi-reference charge-dependent density functional theory and beyond

M. Konieczka,¹ P. Bączyk,¹ and W. Satuła¹

¹*Institute of Theoretical Physics, Faculty of Physics,
University of Warsaw, ul. Pasteura 5, PL-02-093 Warsaw, Poland*

(Dated: November 26, 2021)

Background: Theoretical approaches based on energy density functionals (EDF) are gaining on popularity due to their broad range of applicability. One of their key features is the proper treatment of symmetries of the nuclear interaction. It is because of this that EDF-based methods may provide another independent verification of foundations of the Standard Model, i.e. the assumption that the hadronic structure of matter is indeed built upon three generations of quarks. However, such a study cannot be precisely performed without including very subtle isospin-symmetry-breaking (ISB) terms both in the long- and short-range part of the nuclear interaction. Only very recently has the latter part of ISB interaction been successfully adapted to EDF to describe the Nolen-Schiffer anomaly.

Purpose: The aim of the paper is to study the impact of the short-range ISB terms on isospin impurities in the wave functions of $T = 1/2$ mirrors (α_{ISB}) and the ISB corrections to their Fermi decays (δ_{ISB}). The consequent purpose is to eventually lead the calculation towards evaluation of the V_{ud} matrix element of the Cabbibo-Kobayashi-Maskawa (CKM) quark mixing matrix.

Methods: We use multi-reference density functional theory (MR-DFT) that conserves angular momentum and properly treats isospin. Moreover, for the very first time, the functional includes both short- and long-range isospin-symmetry-breaking forces. Calculations are performed using three different variants of the ISB interaction: (i) involving only the Coulomb force, (ii) involving the Coulomb and leading-order (LO) contact isovector forces, and (iii) involving the Coulomb and next-to-leading-order (NLO) contact isovector forces. The evaluation of the V_{ud} matrix element requires a more subtle approach involving configuration mixing. For this reason, the calculation is performed with a DFT-rooted no core configuration interaction (DFT-NCCI) model including the above-mentioned ISB terms as well.

Results: We compute isospin impurities and ISB corrections in $T = 1/2$ mirrors ranging from $A = 11$ to 47 with MR-DFT formalism. Next, we focus on the best measured $A = 19, 21, 35,$ and 37 mirror pairs, calculate the ISB corrections to their Fermi decays with a DFT-rooted NCCI method, and then extract the V_{ud} matrix element. The final result shows that $V_{ud} = 0.9736(16)$, which (central value) is in good agreement with the value assessed from the superallowed $0^+ \rightarrow 0^+$ Fermi transitions and is only slightly above the value obtained using a state-of-the-art shell model. Last but not least, we demonstrate the stability of our calculation.

Conclusions: The isovector short-range interaction surprisingly strongly influences the isospin impurities and ISB corrections in the $T = 1/2$ mirrors as compared to the calculation in which Coulomb interaction is the only source of isospin-symmetry breaking. Moreover, the V_{ud} matrix element is sensitive to the short-range isovector terms in the interaction and can be successfully extracted within the DFT-rooted approach that includes configuration mixing.

PACS numbers: 21.10.Hw, 21.10.Pc, 21.60.Jz, 21.30.Fe, 23.40.Hc, 24.80.+y

I. INTRODUCTION

With high-precision experiments and theoretical modeling of atomic nuclei one can test fundamental equations governing the properties of subatomic matter. Of particular interest are processes used to search for possible signals of *new physics* beyond the Standard Model (SM), like the superallowed $0^+ \rightarrow 0^+$ β -decays, see [1] and references quoted therein. With small, of order of a percent, theoretical corrections accounting for radiative processes and isospin-symmetry breaking (ISB), these pure Fermi (vector) decays allow verification of the conserved vector current (CVC) hypothesis with a very high precision. In turn, they provide the most precise values of the leading element, V_{ud} , of the Cabbibo-Kobayashi-Maskawa (CKM) matrix.

The mixed Fermi-Gamow-Teller decays of $T = 1/2$

mirror nuclei, which are a subject of this work, offer an alternative way for the SM tests [2, 3] provided that another observable like the β -neutrino correlation (a), β -asymmetry (A), or neutrino-asymmetry (B) coefficient is measured with high accuracy. The SM expressions for a_{SM} , A_{SM} , and B_{SM} can be found, for example, in the review [4]. These coefficients depend on angular momenta of the participating nuclear states and a mixing ratio ϱ of the Gamow-Teller (M_{GT}) and Fermi (M_{F}) matrix elements:

$$\varrho = \frac{g_{\text{A}} M_{\text{GT}}}{g_{\text{V}} M_{\text{F}}}, \quad (1)$$

where $g_{\text{V/A}}$ are vector and axial-vector electroweak currents coupling constants, respectively. Precision measurements of a_{SM} , A_{SM} , or B_{SM} provide, therefore, empirical values of ϱ , which are instrumental for the V_{ud}

calculation because they allow us to avoid using theoretical values of ϱ which, in spite of a recent progress in the *ab initio* GT-decay calculation [5], are not yet accurate enough to be directly used for that purpose. With the experimental ϱ the V_{ud} calculation depends upon precision measurement of the partial lifetime and theoretically calculated radiative ($\delta_R^V, \delta_{NS}^V, \Delta_R^V$) and many-body ISB (δ_{ISB}^V) corrections to the Fermi branch. The latter are defined together with δ_{NS}^V as a deviation from the Fermi matrix element in its isospin-symmetry limit M_F^0 :

$$|M_F|^2 = |M_F^0|^2(1 + \delta_{NS}^V - \delta_{ISB}^V) \quad (2)$$

Indeed, the reduced lifetime for an allowed semileptonic β -decay of $T = 1/2$ mirror nuclei can be written as [2, 3]:

$$\begin{aligned} \mathcal{F}t^{\text{mirror}} &\equiv f_V t(1 + \delta_R^V)(1 + \delta_{NS}^V - \delta_{ISB}^V) \\ &= \frac{K}{G_F^2 V_{ud}^2 C_V^2 (1 + \Delta_R^V) \left(1 + \frac{f_A}{f_V} \varrho^2\right)}, \end{aligned} \quad (3)$$

where $K/(\hbar c)^6 = 2\pi^3 \hbar \ln 2 / (m_e c^2)^5 = 8120.2787(11) \times 10^{-10} \text{ GeV}^{-4} \text{ s}$ is a universal constant, G_F is the Fermi-decay coupling constant $G_F/(\hbar c)^3 = 1.16637(1) \times 10^{-5} \text{ GeV}^{-2}$, and $f_{V/A}$ denotes the phase space factors. Hence, similar to the superallowed $0^+ \rightarrow 0^+$ decays, the quality of the test depends on the accuracy of empirical data and the quality of the theoretical models used to compute the corrections, in particular the many-body δ_{ISB}^V corrections which are a subject of this work. Current precision of $T = 1/2$ mirror decay experiments is achieved only for a handful of isotopes, which is still not enough for stringent testing of the SM. However, fast progress in β -decay correlation techniques opens up new opportunities and keeps the field vibrant; see, for example, Ref. [6] for the recent high-precision β -asymmetry measurement in ^{37}K decay.

The goal of this work is to study the impact of isovector effective contact interaction that is adjusted to account for the Nolen-Schiffer anomaly [7] in nuclear masses on isospin impurities in the wave functions of $T = 1/2$ mirrors, the isospin symmetry breaking (ISB) corrections to their Fermi decays, and the V_{ud} matrix element in *sd*-shell $T = 1/2$ mirror nuclei. We use different variants of symmetry-restored density functional theory (DFT) which were successfully applied in the past to compute isospin impurities and ISB corrections to super-allowed $0^+ \rightarrow 0^+$ decays, see [8, 9]. After a brief presentation of the methods in Sect. II we demonstrate that the class-III local force strongly affects the calculated isospin impurities, see Sect. III A. This rather counterintuitive observation motivated us to undertake a detailed theoretical study of the ISB corrections to the Fermi branch of $T = 1/2$ ground state decays. In this context, in the first place, we present isospin and angular-momentum projected multi-reference DFT calculations covering $T = 1/2$ nuclei with $11 \leq A \leq 47$, see Sect. III A. Next, in

Sect. III B, we focus on decays of $A=19, 21, 35$, and 37 mirror nuclei for which experimental data on correlation parameters are precise enough to allow for extraction of the V_{ud} matrix element. For these cases we perform the DFT-based No-Core-Configuration-Interaction calculations (DFT-NCCI), see [10] for details, including theoretical uncertainty analysis, see Sect. III C. The paper is summarized in Sect. IV.

II. METHODS

The nuclear mean-field-based models are almost perfectly tailored to study the ISB effects. The single-reference DFT (SR-DFT) treats Coulomb polarization properly, without involving an approximation of an inert core, and accounts for an interplay between short- and long-range forces in a self-consistent way. The spontaneous symmetry breaking (SSB) effects that accompany the SR-DFT solutions and introduce, in particular, spurious isospin impurities and angular-momentum non-conservation can be then taken care of by extending the framework beyond mean field to multi-reference level (MR-DFT) with the aid of isospin- and angular-momentum projection techniques [8, 9, 11]. However, the nuclear energy density functionals (EDF) which are conventionally applied in the DFT-based calculations use Coulomb as the only source of ISB. Therefore they are incomplete in the context of the ISB studies and cannot fully describe ISB observables like Triplet (TDE) or Mirror Displacement Energies (MDE) of nuclear binding energies. The latter deficiency is known in the literature as the Nolen-Schiffer anomaly [7]. There is a consensus that these deficiencies cannot be cured without introducing non-Coulombic sources of ISB as shown within the nuclear shell model (NSM), Hartree-Fock (HF) theory or *ab initio* calculations in Refs. [12–19] and references given therein.

Recently, we constructed a single-reference charge-dependent DFT (SR-CDDFT) that includes, apart of the Coulomb and isoscalar Skyrme interactions, the leading-order (LO) zero-range and next-to-leading-order (NLO) gradient interactions of class II, which introduces charge-independence breaking (CIB) and class III describing charge-symmetry-breaking (CSB) effects in the Henley and Miller classification [20, 21]. We subsequently demonstrated that the SR-CDDFT allows for very accurate treatment of MDEs and TDEs in a very broad range of masses already in LO [22] and showed that the description can be further improved by adding NLO terms [23]. In Ref. [23] we also provide arguments that the newly introduced ISB terms model strong-force-related effects of CIB and CSB rather than the beyond-mean-field electromagnetic corrections.

The aim of this work is to extend the SR-CDDFT to MR-CDDFT and perform a systematic study of the isospin impurities and ISB corrections to the beta decays in $T = 1/2$ mirrors. In this case the ISB effects due

to class II or class IV forces are negligible [16, 22, 23]. Therefore, the non-Coulombic ISB force can be approximated by the isovector effective interaction up to NLO in the effective theory expansion:

$$\hat{V}^{\text{III}}(i, j) = \left(t_0^{\text{III}} \delta(\mathbf{r}_{ij}) + \frac{1}{2} t_1^{\text{III}} [\delta(\mathbf{r}_{ij}) \mathbf{k}^2 + \mathbf{k}'^2 \delta(\mathbf{r}_{ij})] + t_2^{\text{III}} \mathbf{k}' \delta(\mathbf{r}_{ij}) \mathbf{k} \right) \left(\hat{\tau}_3^{(i)} + \hat{\tau}_3^{(j)} \right) \quad (4)$$

where $\mathbf{k} = \frac{1}{2i} (\nabla_i - \nabla_j)$ ($\mathbf{k}' = -\frac{1}{2i} (\nabla_i - \nabla_j)$) are relative momentum operators acting to the right (left), respectively.

The essence of MR-DFT is to cure the spurious effects of SSB. The procedure boils down to a re-diagonalization of the entire Hamiltonian in a good-isospin and good angular-momentum basis generated by acting on the HF configuration $|\varphi\rangle$ with the standard 1D isospin $\hat{P}_{T_z T_z}^T$ and 3D angular-momentum \hat{P}_{MK}^I projection operators:

$$|\varphi; IMK; TT_z\rangle = \frac{1}{\sqrt{N_{\varphi; IMK; TT_z}}} \hat{P}_{T_z T_z}^T \hat{P}_{MK}^I |\varphi\rangle. \quad (5)$$

Due to overcompleteness of the set (5), the re-diagonalization of the Hamiltonian is performed by solving the Hill-Wheeler-Griffin equation in the *collective space* – a subspace spanned by the linearly independent *natural states* $|\varphi; IM; TT_z\rangle^{(i)}$ accounting for the K -mixing, see Ref. [24] for further details. The resulting eigenfunctions are:

$$|n; \varphi; IM; T_z\rangle = \sum_{i, T \geq |T_z|} b_{iT}^{(nI; \varphi)} |\varphi; IM; TT_z\rangle^{(i)}, \quad (6)$$

where n enumerates eigenstates in ascending order according to their energies. The quantum state (6) is free from spurious isospin mixing. It has to be noted, however, that it may not be equipped with the correlation coming from higher excitations. Such a lack can be compensated by applying configuration mixing in DFT-NCCI formalism.

The DFT-NCCI scheme proceeds as follows. One starts with computation of relevant (multi)particle-(multi)hole deformed HF configurations φ_i . Next, with the aid of projection methods, one computes a set of projected states $|\varphi_i; IMK; TT_z\rangle$, see Eq. (5), which are subsequently mixed to account for K -mixing and physical isospin-mixing. At this stage one obtains a set of non-orthogonal states $|n; \varphi_i; IM; T_z\rangle$ of Eq. (6), which are eventually mixed by solving the Hill-Wheeler-Griffin equation. In the mixing we use the same Hamiltonian that was used to create the HF configurations. Further details concerning the DFT-NCCI scheme can be found in Ref. [10].

All calculations presented below were done using the code HFODD [25] with the SV_{SO} Skyrme force, a variant of the SV EDF of Ref. [26] with the tensor terms included and the spin-orbit strength increased by a factor of 1.2 as proposed in Ref. [27]. The code includes the local ISB

EDF, in the LO and NLO variants, and allows for simultaneous 1D isospin and 3D angular-momentum projections, and is also equipped with the DFT-NCCI module. In the following we compare three variants of the calculations including different ISB forces: (i) involving only the Coulomb force (\hat{V}_C), (ii) involving the Coulomb and LO contact ISB forces ($\hat{V}_C + \hat{V}_{\text{LO}}^{\text{III}}$), and (iii) involving the Coulomb and NLO local ISB forces ($\hat{V}_C + \hat{V}_{\text{NLO}}^{\text{III}}$). These variants will be labeled by the acronyms C, LO, and NLO, respectively.

III. RESULTS

A. The influence of zero-range isovector interaction on isospin impurities and ISB corrections to Fermi β -decays

The contribution to MDE in $T=1/2$ mirror nuclei due to the contact class-III interaction constitutes, on average, around 7 to 8% of the contribution coming from the Coulomb force, as shown in Refs. [22, 23]. One would therefore naively expect that the class-III ISB force would also have a rather modest impact on the isospin impurity in the n -th state of spin I : $\alpha_{\text{ISB}}^{(n)} = 1 - \sum_i |b_{iT=|T_z|}^{(nI; \varphi)}|^2$. Figure 1 shows arithmetic means

$$\bar{\alpha}_{\text{ISB}}(A) = [\alpha_{\text{ISB}}(A, T_z = 1/2) + \alpha_{\text{ISB}}(A, T_z = -1/2)]/2$$

in the ground states of $T_z = \pm 1/2$ for $11 \leq A \leq 47$. The curves illustrate impurities obtained using C (α_C), LO (α_{LO}), and NLO (α_{NLO}) variants of the ISB interaction with parameters taken from [23].

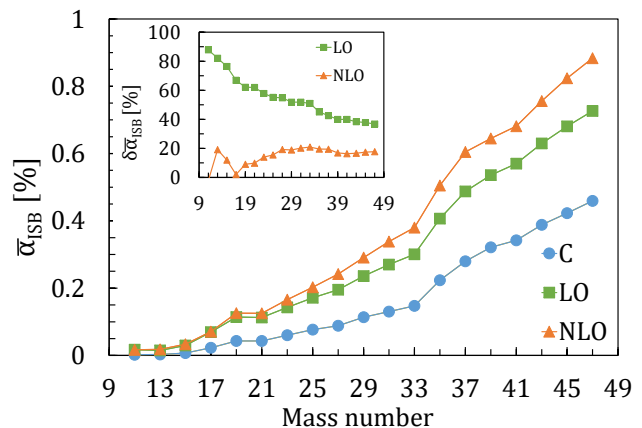


FIG. 1. (Color online) Arithmetic means of $\bar{\alpha}_C$ (blue), $\bar{\alpha}_{\text{LO}}$ (green), and $\bar{\alpha}_{\text{NLO}}$ (orange) over the ground-state values in $T_z = \pm 1/2$ mirror partners versus A . The insert shows relative differences $\delta\bar{\alpha}_{\text{LO}} \equiv \frac{\bar{\alpha}_{\text{LO}} - \bar{\alpha}_C}{\bar{\alpha}_{\text{LO}}}$ and $\delta\bar{\alpha}_{\text{NLO}} \equiv \frac{\bar{\alpha}_{\text{NLO}} - \bar{\alpha}_{\text{LO}}}{\bar{\alpha}_{\text{NLO}}}$.

It is surprising to see that the local class-III force strongly increases isospin mixing. The relative difference

between α_{LO} and α_{C} gradually decreases with A (see insert in Fig. 1) from 90% to circa 40% (50%) in the lower fp -shell nuclei for the LO (NLO) theory, respectively. Note also that the NLO theory brings a much smaller increase of α_{ISB} as compared to the LO, which is expected for a converging effective theory. We have also verified (using isospin-projected theory) that a strong increase in α_{ISB} due to class-III force takes place for density-dependent popular Skyrme forces like SLy4 [28].

The additional isospin mixing introduced by ISB contact terms, see Eq. (4), is expected to impact the ISB corrections to the Fermi branch in mirror β -decays. In order to assess the effect quantitatively, we performed systematic calculation of $\delta_{\text{ISB}}^{\text{V}}$ in $11 \leq A \leq 47$ using the SV_{SO} Skyrme force and three variants C, LO, and NLO of the ISB forces. Because the precision is of the utmost importance, we refitted the class-III ISB interaction and adjusted its parameters to MDEs in $11 \leq A \leq 47$ calculated at the MR-DFT level. The fit gives $t_0^{\text{III}} = -6.3 \pm 0.3$ MeV fm³ for the $\text{SV}_{\text{SO}}^{\text{LO}}$ functional and $t_0^{\text{III}} = 0 \pm 2$ MeV fm³, $t_1^{\text{III}} = -2 \pm 2$ MeV fm⁵, and $t_2^{\text{III}} = -4 \pm 1$ MeV fm⁵ for the $\text{SV}_{\text{SO}}^{\text{NLO}}$ functional. In the latter case we observed that the t_0^{III} and t_1^{III} parameters are strongly correlated, which increases their theoretical uncertainty and, in turn, the uncertainty on the calculated $\delta_{\text{ISB}}^{\text{V}}$. The results of the $\delta_{\text{ISB}}^{\text{V}}$ calculation are presented in Fig. 2. As anticipated, an enhancement in α_{ISB} implies strong enhancement in $\delta_{\text{ISB}}^{\text{V}}$, of the order of 70% on average, caused by the LO term and further, albeit as expected much smaller, increase obtained in the NLO calculation.

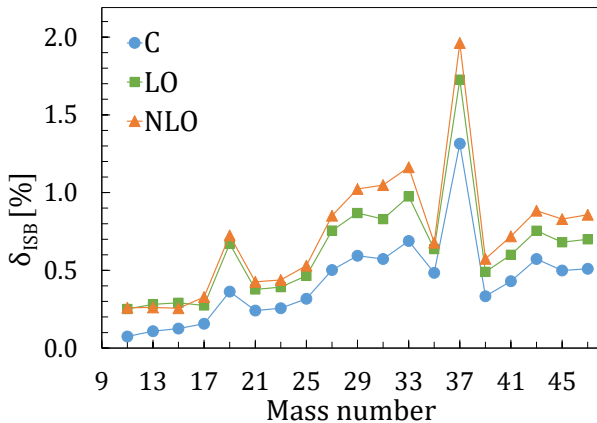


FIG. 2. (Color online) ISB corrections to the Fermi branch of ground-state beta decay in $T = 1/2$ mirror nuclei calculated using variants C (blue dots), LO (green squares), and NLO (orange triangles) of our MR-DFT model.

B. Evaluation of the V_{ud} matrix element in DFT-NCCI calculation

The calculated $\delta_{\text{ISB}}^{\text{V}}$ versus the A curve shows two irregularities for $A=19$ and $A=37$. Such irregularities indicate enhanced mixing among single-particle Nilsson orbitals and, indirectly, suggest that the MR-DFT calculations are not sufficient. Similar problems were encountered already in our seminal MR-DFT calculation of $\delta_{\text{C}}^{\text{V}}$ for $0^+ \rightarrow 0^+$ superallowed Fermi decays in $A = 38$ (and $A = 18$) cases, see Ref. [9]. The value of $\delta_{\text{C}}^{\text{V}}$ calculated in Ref. [9] for $A = 38$ was anomalously large due to accidental near-degeneracy and very strong mixing of the Nilsson orbitals originating from the $1s_{1/2}$ and $0d_{3/2}$ spherical sub-shells. Within the MR-DFT framework (involving projection from a single Slater determinant) such an anomalous case must be treated as an outlier and removed from further analysis of V_{ud} , which was in fact done in Ref. [9]. At the MR-DFT level of approximation there is no cure for such an effect. Hence, the large values of $\delta_{\text{ISB}}^{\text{V}}$ for $A = 37$ and, to a lesser extent, for $A = 19$ mirror decays, caused by the same $1s_{1/2} - 0d_{3/2}$ unphysical mixing, should also be rejected from further analysis of V_{ud} . This, in turn, would limit the V_{ud} analysis within the MR-DFT to the two well-measured cases only, making the entire procedure statistically questionable.

With the development of DFT-NCCI [10], however, we have at our disposal a new theoretical tool which allows us to control, at least to some extent, such an unwanted mixing. The model provides re-diagonalization of the entire Hamiltonian within the model space that includes the interacting mean-field configurations. We, therefore, decided to analyze all four well measured $A=19, 21, 35,$ and 37 mirror decays using this formalism. Moreover, in the present work DFT-NCCI calculations were limited to one-particle-one-hole ($p-h$) configurations only. Such an approach was widely tested in our previous beta-decay calculation reported in [29]. The calculated ground-state (gs) and excited $p-h$ configurations in the four mirror nuclei are axially deformed, which implies that the number of participating $p-h$ configurations is very limited due to the K quantum number conservation. In such a case, the configuration mixing, which proceeds through a spherically symmetric Hamiltonian, is effective only within the collective subspace built upon HF configurations of the same K . In $A=19$ and $A=37$ the gs configuration is built upon the $K=1/2$ Nilsson state with spin $I=1/2$ and $I=3/2$, respectively. Hence, the mixing is effective within three HF configurations having $\Delta K = 0$. These configurations are built upon one of the three active $K=1/2$ Nilsson orbits [220 1/2], [200 1/2], and [211 1/2] originating from the $d_{5/2}$, $s_{1/2}$, and $d_{3/2}$ spherical sub-shells, respectively. In $A=21$ and $A=35$ the gs spin is $I=K=3/2$. The active model space then consists of only two HF configurations built upon either the [211 3/2] or [202 3/2] Nilsson orbits originating from $d_{5/2}$ and $d_{3/2}$ spherical subshells.

The large energy gap between the [211 3/2] or [202 3/2]

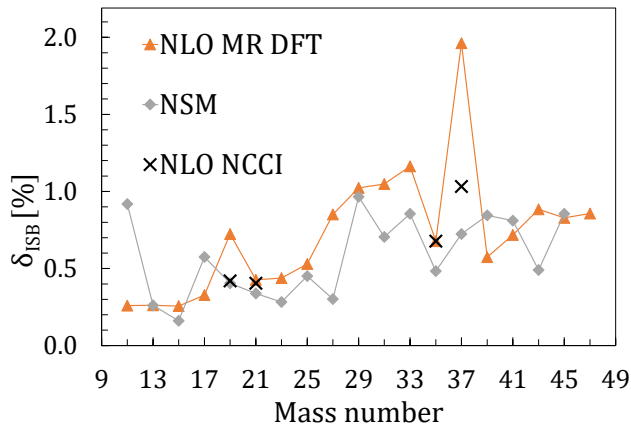


FIG. 3. (Color online) ISB corrections to the Fermi branch of ground-state beta decay in $T = 1/2$ mirror nuclei calculated using NLO (orange triangles) of our MR-DFT model in comparison with the nuclear shell model (NSM) results (grey diamonds) taken from Ref. [2]. Black crosses mark the DFT-NCCI results for $A=19, 21, 35,$ and 37 decays, see Tab. I.

Nilsson orbits decreases considerably the effect of configuration mixing on $\delta_{\text{ISB}}^{\text{V}}$ in $A=21$ and $A=35$. In contrast, the effect is very strong in $A=19$ and $A=37$. For the $^{19}\text{Ne} \rightarrow ^{19}\text{F}$, in the NLO variant, the ISB correction $\delta_{\text{ISB}}^{\text{V}}$ drops from 0.738% calculated for the single configuration representing the ground state to 0.580% after admixing the first excited configuration, and further to 0.430% after admixing the second excited configuration. For the $^{37}\text{K} \rightarrow ^{37}\text{Ar}$ decay the ISB correction decreases from 1.833% to 1.099% and down to 1.042%, respectively. Note that the configuration mixing in $A=19$ and 37 corrects, to a large extent, the irregular behavior of $\delta_{\text{ISB}}^{\text{V}}$ versus A obtained for these two cases in MR-DFT, see Fig. 3.

TABLE I. ISB corrections $\delta_{\text{ISB}}^{\text{V}}$ to the Fermi transitions in $A=19, 21, 35,$ and 37 calculated using the NSM [2] and the C, LO, and NLO variants of the DFT-NCCI model. The last three rows show the results for $\bar{\mathcal{F}}t_0$, V_{ud} , and for the unitarity test obtained by averaging over the results in $A=19, 21, 35,$ and 37 .

A	NSM	C	LO	NLO
19	0.415(39)	0.231(30)	0.412(54)	0.430(56)
$\delta_{\text{ISB}}^{\text{V}}$ 21	0.348(27)	0.251(33)	0.394(50)	0.415(54)
35	0.493(46)	0.474(62)	0.647(84)	0.688(89)
37	0.734(61)	0.714(93)	0.97(13)	1.04(14)
$\bar{\mathcal{F}}t_0$	6162(15)	6166(18)	6156(18)	6152(21)
V_{ud}	0.9727(14)	0.9725(14)	0.9732(14)	0.9736(16)
unitarity	0.9967(31)	0.9961(31)	0.9976(31)	0.9983(35)

Table I summarizes the results of DFT-NCCI calcula-

tions. It contains the results for the calculated values of $\delta_{\text{ISB}}^{\text{V}}$, the average values of nucleus-independent reduced-lifetime $\bar{\mathcal{F}}t_0$ defined, for a single transition, as:

$$\mathcal{F}t_0 \equiv \mathcal{F}t^{\text{mirror}} \left(1 + \frac{f_A}{f_V} \rho^2 \right), \quad (7)$$

the extracted values of V_{ud} , and the result of the unitarity test. Note that the DFT-NCCI theory for V_{ud} is convergent with respect to the addition of higher order ISB terms as depicted in Fig. 4, and that the final V_{ud} matrix element

$$V_{\text{ud}} = 0.9736 \pm 0.0016$$

lies within $\frac{1}{2}\sigma$ of the value assessed from superallowed $0^+ \rightarrow 0^+$ Fermi transitions, which is $V_{\text{ud}} = 0.97417 \pm 0.00021$ [1]. In the calculations of $\bar{\mathcal{F}}t_0$ and V_{ud} we used the radiative corrections and phase-space factors taken from Ref. [2]. The experimental data were taken from Ref. [30, 31] in the case of $A=19$ in which we have taken an error-weighted sum of a half-life time reported from these independent experiments; the same for $A = 21$ [32, 33], $A = 35$ [3], and for $A = 37$ [6].

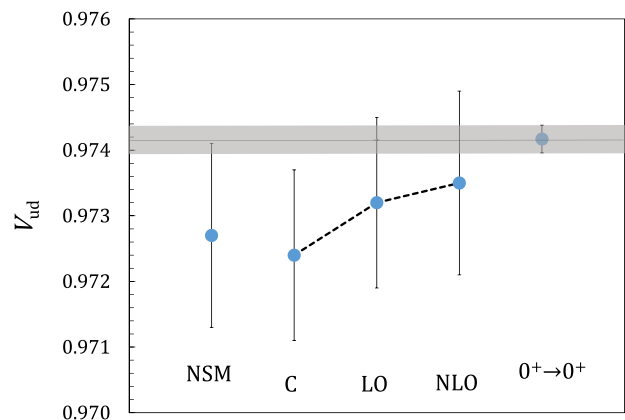


FIG. 4. (Color online) V_{ud} matrix element calculated from the $T = 1/2, A = 19, 21, 35,$ and 37 mirror decays by means of the NSM [2] and the three variants C, LO, and NLO of the DFT-NCCI model. Right point represents the V_{ud} obtained from superallowed Fermi beta decays taken from Ref. [1].

C. Theoretical uncertainty analysis

Let us finally comment on theoretical uncertainties. The overall uncertainty imposed on the calculated ISB comes from three major sources: (i) from the cut-off on a harmonic oscillator basis, (ii) from the uncertainties of the class-III LECs, and finally (iii) from the configuration mixing. The uncertainties associated with the first two sources can be reliably estimated and do not exceed $\sim 5\%$. The uncertainty associated with configuration mixing can be evaluated only *a posteriori*, after

performing configuration-interaction calculations in the larger configuration space.

In order to assess the uncertainty associated with configuration mixing we decided to perform configuration-interaction calculations for two representative cases $A = 21$ and $A = 37$. In the case of $^{21}\text{Na} \rightarrow ^{21}\text{Ne}$ decay we increased the model space to 12 axially deformed configurations, which are depicted schematically in Tab. II. The result of the calculation is shown in Fig. 5. The figure presents a relative change in the calculated ISB correction with respect to the value quoted in Tab. I. As shown in the figure, admixture of seniority one 1p–1h excitations (configurations no 1-5) does not bring any relevant effect on δ_{ISB} . A perceptible increase can be noticed after admixing of nn -, pp -, and np - pairing-type 2p–2h excitations in the configuration space. The amount of the increase is around 5%, which means that for this, and most likely, also for the $A=35$ case, our predictions can be considered as very stable with respect to the configuration mixing.

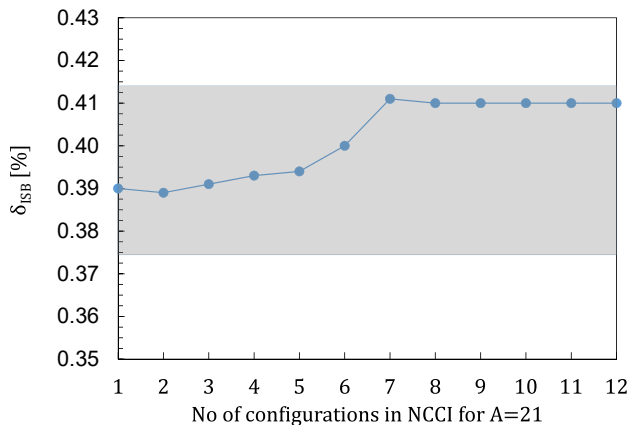


FIG. 5. (Color online) ISB correction to the Fermi transition $^{21}\text{Na} \rightarrow ^{21}\text{Ne}$ with respect to an increase of a configuration space involving 1p–1h and 2p–2h pairing-type excitations. Configurations are added in the order listed in Table II. Shaded area marks 5% error bar superimposed on the DFT-NCCI result calculated using 1p-1h configurations. The calculation was performed for the LO variant of the isovector interaction, see Eq. (4) using the single-particle basis consisting of $N = 12$ harmonic oscillators shells.

We performed a similar calculation for the irregular and therefore most difficult case of $^{37}\text{K} \rightarrow ^{37}\text{Ar}$ transition. In the analysis we included seven configurations depicted in Table III. The calculation indicates (see Fig. 6) that the total estimated error due to configuration mixing in this case is of the order of 15%. It might be even slightly larger after including more 2p–2h excitations. However, the proximity of Nilsson orbitals provoking unstable HF solutions disables performance of such analysis. Nevertheless, at the moment, there is no strong motivation to conducting such a study. The theoretical error associated with the δ_{ISB} calculation constitutes only a tiny fraction

in the total error budget of $|V_{\text{ud}}|$, which is completely dominated by experimental uncertainties [3]. In conclusion, we have imposed a 15% error on our irregular δ_{ISB} in $A = 19$ and $A = 37$ and a 5% error in regular $A = 21$ and $A = 35$ cases due to configuration mixing.

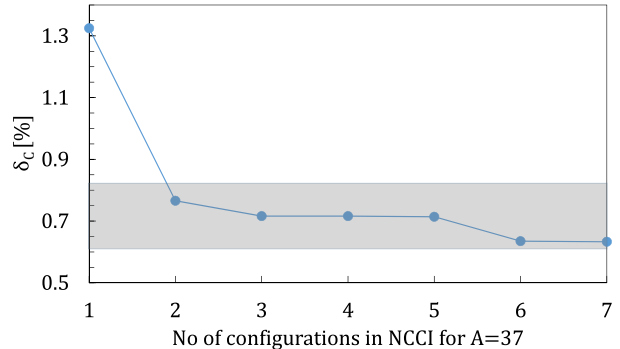


FIG. 6. (Color online) ISB correction to the Fermi transition $^{37}\text{K} \rightarrow ^{37}\text{Ar}$ with respect to an increase of a configuration space involving 1p–1h and 2p–2h pairing-type excitations. Configurations are added in the order listed in Table III. Shaded area marks 15% error bar superimposed on the DFT-NCCI result calculated using 1p-1h configurations. The calculation was performed using the single-particle basis consisting of $N = 12$ harmonic oscillators shells with the Coulomb as the only source of isospin-symmetry breaking.

Let us finally mention that our results are obviously a subject to systematic error associated with the form and parameters of the employed EDF. Our earlier calculations (see Ref. [11]) as well as the random-phase approximation calculations by Liang *et al.* [34] suggest that variations in EDF parameterizations should rather weakly influence the extracted V_{ud} . Detailed analysis of such uncertainties, however, is very difficult and will not be performed here. As already mentioned, the total error budget of $|V_{\text{ud}}|$ is, at present, dominated by experimental uncertainties [3].

IV. CONCLUSIONS

In this paper, we have performed a systematic study of isospin impurities to the nuclear wave functions in $T=1/2$ mirror nuclei using MR-CDDFT, which includes, apart from the Coulomb interaction, the class-III ISB interaction adjusted to reproduce the Nolen-Schiffer anomaly in MDEs. We have investigated the impurities using three variants of the model including different ISB forces, namely: (i) involving only the Coulomb force, (ii) involving the Coulomb and LO contact ISB forces, and (iii) involving the Coulomb and local ISB forces up to NLO. We have demonstrated, for the first time, that the class-III interaction very strongly increases the isospin mixing,

TABLE II. (Color online) Configurations used in the DFT-NCCI calculations for $A=21$ mirrors. Full dots denote pairwise occupied Nilsson states. Up (down) arrows denote singly occupied Nilsson states with positive (negative) K quantum numbers, respectively. Note that excitation of a pair to the $|202\ 5/2\rangle$ Nilsson level leads to oblate shape.

group	PROLATE									group	OBLATE			
config.	g.s.	$\nu = 1$					nn/pp	np	nn/pp	$\nu = 3$	config.	g.s.	nn/pp	np
total K	3/2	1/2	1/2	1/2	3/2	3/2	3/2	3/2	3/2	3/2	total K	3/2	3/2	3/2
kernel	1	2	3	4	5	6	7	8	9	kernel	10	11	12	
$ 202\ 3/2\rangle$														
$ 211\ 1/2\rangle$														
$ 200\ 1/2\rangle$														
$ 202\ 5/2\rangle$														
$ 211\ 3/2\rangle$														
$ 220\ 1/2\rangle$														

TABLE III. (Color online) Configurations used in the DFT-NCCI calculations for $A=37$ mirrors. Full dots denote pairwise occupied Nilsson states. Up (down) arrows denote singly occupied Nilsson states with positive (negative) K quantum numbers, respectively.

group	OBLATE							
config.	g.s.	$\nu = 1$					nn/pp	$\nu = 3$
total K	1/2	3/2	1/2	1/2	3/2	1/2	1/2	
kernel	1	2	3	4	5	6	7	
$ 211\ 1/2\rangle$								
$ 202\ 3/2\rangle$								
$ 200\ 1/2\rangle$								
$ 220\ 1/2\rangle$								
$ 211\ 3/2\rangle$								
$ 202\ 5/2\rangle$								

see Fig. 1. Our results show that the NLO theory is convergent and brings a much smaller increase of α_{ISB} as compared to the LO theory.

Next, we have presented a profound impact of class-III force on the isospin-symmetry-breaking corrections $\delta_{\text{ISB}}^{\text{V}}$ to the Fermi matrix elements of ground-state decays of $T=1/2$ mirror nuclei, which constitute a theoretical input for the precision tests of the electroweak sector of the SM. In order to assess the effect quantitatively we have performed a systematic study of $\delta_{\text{ISB}}^{\text{V}}$ using MR-DFT with the three variants of the ISB force described above. As expected from the α_{ISB} study, we have observed a strong systematic increase in $\delta_{\text{ISB}}^{\text{V}}$ after including the LO class-III force and a further, albeit much smaller, increase within the NLO theory.

The $\delta_{\text{ISB}}^{\text{V}}$ calculated using MR-DFT shows irregularities for $A=19$ and 37 cases, which are among the decays that are used for the SM test. Such irregularities

usually indicate a mixing among the active Nilsson orbitals, which can be taken care of by performing configuration-interaction calculations. In order to verify this conjecture and make our predictions more precise we performed the DFT-NCCI calculations of the ISB corrections in $A=19, 21, 35,$ and 37 $T = 1/2$ mirrors. Because these nuclei are axial we have limited the DFT-NCCI model space to particle-hole deformed Nilsson configurations with $\Delta K=0$, with respect to the K quantum number of the ground-state configuration. The DFT-NCCI results are shown in Tab. I. The values of $\delta_{\text{ISB}}^{\text{V}}$ calculated using the LO and NLO theories are systematically larger than the results obtained using only the Coulomb interaction. They are also systematically larger than the corrections calculated using the NSM in Ref. [2]. In turn, the extracted central value of V_{ud} matrix element is closer to the value obtained using data on $0^+ \rightarrow 0^+$. Our $|V_{\text{ud}}|=0.9736(16)$ was obtained with the error-weighted average over four mirror ($A=19, 21, 35,$ and 37) transitions excluding the outlier $A=29$, a case measured with lower accuracy as compared to other cases, see [3]. This value is considerably larger than $|V_{\text{ud}}|=0.9727(14)$, given in Ref. [6] and above the value $|V_{\text{ud}}|=0.9730(14)$ of Ref. [35], which includes also the $A=29$ decay in the average.

ACKNOWLEDGMENTS

This work was supported in part by the Polish National Science Centre under Contract Nos. 2017/24/T/ST2/00160 and 2018/31/B/ST2/02220. We acknowledge CIŚ Świerk Computing Center, Poland, for the allocation of computational resources.

- [1] J. C. Hardy and I. S. Towner, Phys. Rev. C **91**, 025501 (2015).
 [2] N. Severijns, M. Tandecki, T. Phalet, and I. S. Towner, Phys. Rev. C **78**, 055501 (2008).

- [3] O. Naviliat-Cuncic and N. Severijns, Phys. Rev. Lett. **102**, 142302 (2009).
 [4] N. Severijns, M. Beck, and O. Naviliat-Cuncic, Rev. Mod. Phys. **78**, 991 (2006).

- [5] P. Gysbers *et al.*, Nature Physics **15**, 428 (2019).
- [6] B. Fenker, A. Gorelov, D. Melconian, J. Behr, M. Anholm, D. Ashery, R. Behling, I. Cohen, I. Craiciu, *et al.*, Phys. Rev. Lett. **120**, 062502 (2018).
- [7] J. A. Nolen, Jr and J. P. Schiffer, Ann. Rev. Nucl. Sci. **19**, 471 (1969).
- [8] W. Satuła, J. Dobaczewski, W. Nazarewicz, and M. Rafalski, Phys. Rev. Lett. **103**, 012502 (2009).
- [9] W. Satuła, J. Dobaczewski, W. Nazarewicz, and M. Rafalski, Phys. Rev. Lett. **106**, 132502 (2011).
- [10] W. Satuła, P. Bączyk, J. Dobaczewski, and M. Konieczka, Phys. Rev. C **94**, 024306 (2016).
- [11] W. Satuła, J. Dobaczewski, W. Nazarewicz, and M. Rafalski, Phys. Rev. C **81**, 054310 (2010).
- [12] W. Ormand and B. Brown, Nucl. Phys. A **491**, 1 (1989).
- [13] T. Suzuki, H. Sagawa, and N. Van Giai, Phys. Rev. C **47**, R1360 (1993).
- [14] B. A. Brown, W. A. Richter, and R. Lindsay, Physics Letters B **483**, 49 (2000).
- [15] A. P. Zuker, S. M. Lenzi, G. Martinez-Pinedo, and A. Poves, Phys. Rev. Lett. **89**, 142502 (2002).
- [16] J. Carlson, S. Gandolfi, F. Pederiva, S. C. Pieper, R. Schiavilla, K. E. Schmidt, and R. B. Wiringa, Rev. Mod. Phys. **87**, 1067 (2015).
- [17] A. Petrovici, Phys. Rev. C **91**, 014302 (2015).
- [18] K. Kaneko, Y. Sun, T. Mizusaki, S. Tazaki, and S. Ghorui, Physics Letters B **773**, 521 (2017).
- [19] X. Roca-Maza, G. Colò, and H. Sagawa, Phys. Rev. Lett. **120**, 202501 (2018).
- [20] E. M. Henley and G. A. Miller, *Mesons in Nuclei*, edited by M. Rho and D. H. Wilkinson (North Holland, 1979).
- [21] G. A. Miller and W. H. T. van Oers, *Symmetries and Fundamental Interactions in Nuclei*, edited by W. C. Haxton and E. M. Henley (World Scientific, 1995).
- [22] P. Bączyk, J. Dobaczewski, M. Konieczka, W. Satuła, T. Nakatsukasa, and K. Sato, Phys. Lett. B **778**, 178 (2018).
- [23] P. Bączyk, W. Satuła, J. Dobaczewski, and M. Konieczka, J. Phys. G: Nucl. Part. Phys. **46**, 03LT01 (2019).
- [24] J. Dobaczewski, W. Satuła, B. Carlsson, J. Engel, P. Olbratowski, P. Powalowski, M. Sadziak, J. Sarich, N. Schunck, A. Staszczak, M. Stoitsov, M. Zalewski, and H. Zduńczuk, Comput. Phys. Commun. **180**, 2361 (2009).
- [25] N. Schunck, J. Dobaczewski, W. Satuła, P. Bączyk, J. Dudek, Y. Gao, M. Konieczka, K. Sato, Y. Shi, X. Wang, and T. Werner, Computer Physics Communications **216**, 145 (2017).
- [26] M. Beiner, H. Flocard, N. Van Giai, and P. Quentin, Nucl. Phys. A **238**, 29 (1975).
- [27] M. Konieczka, P. Bączyk, and W. Satuła, Phys. Rev. C **93**, 042501(R) (2016).
- [28] E. Chabanat, P. Bonche, P. Haensel, J. Meyer, and R. Schaeffer, Nucl. Phys. A **627**, 710 (1997).
- [29] M. Konieczka, M. Kortelainen, and W. Satuła, Phys. Rev. C **97**, 034310 (2018).
- [30] S. Triambak, P. Finlay, C. S. Sumithrarachchi, G. Hackman, G. C. Ball, and *et al.* Garrett, Phys. Rev. Lett. **109**, 042301 (2012).
- [31] L. Broussard, H. Back, M. Boswell, A. Crowell, P. Dendooven, G. Giri, C. Howell, M. Kidd, K. Jungmann, *et al.*, Phys. Rev. Lett. **112**, 212301 (2014).
- [32] J. Grinyer *et al.*, Phys. Rev. C **91**, 032501(R) (2015).
- [33] P. Shidling, R. Behling, B. Fenker, J. Hardy, V. Iacob, M. Mehlman, H. Park, B. Roeder, D. Melconian, *et al.*, Phys. Rev. C **98**, 015502 (2018).
- [34] H. Liang, N. V. Giai, and J. Meng, Phys. Rev. C **79**, 064316 (2009).
- [35] M. Gonzalez-Alonso, O. Naviliat-Cuncic, and N. Severijns, Prog. Part. Nucl. Phys. **104**, 165 (2019).